

Lab on a Chip

Accepted Manuscript



This is an *Accepted Manuscript*, which has been through the Royal Society of Chemistry peer review process and has been accepted for publication.

Accepted Manuscripts are published online shortly after acceptance, before technical editing, formatting and proof reading. Using this free service, authors can make their results available to the community, in citable form, before we publish the edited article. We will replace this *Accepted Manuscript* with the edited and formatted *Advance Article* as soon as it is available.

You can find more information about *Accepted Manuscripts* in the [Information for Authors](#).

Please note that technical editing may introduce minor changes to the text and/or graphics, which may alter content. The journal's standard [Terms & Conditions](#) and the [Ethical guidelines](#) still apply. In no event shall the Royal Society of Chemistry be held responsible for any errors or omissions in this *Accepted Manuscript* or any consequences arising from the use of any information it contains.

PAPER

An array microhabitat system for high throughput studies of microalgal growth under controlled nutrient gradients

Cite this: DOI: 10.1039/x0xx00000x

Received 00th January 2012,
Accepted 00th January 2012

DOI: 10.1039/x0xx00000x

www.rsc.org/

Beum Jun Kim,^a Lubna V. Richter,^a Nicholas Hatter,^a Chih-kuan Tung,^a Beth A. Ahner,^a and Mingming Wu^a

Microalgae have been increasingly recognized in the fields of environmental and biomedical engineering because of its use as base materials for biofuels or biomedical products, and also the urgent needs to control harmful algal blooms protecting water resources worldwide. Central to the theme is the growth rate of microalgae under the influences of various environmental cues including nutrients, pH, oxygen tension and light intensity. Current microalgal culture systems, e.g. raceway ponds or chemostats, are not designed for system parameter optimizations of cell growth. In this article, we present the development of an array microfluidic system for high throughput studies of microalgal growth under well defined environmental conditions. The microfluidic platform consists of an array of microhabitats flanked by two parallel side channels, all of which are patterned in a thin agarose gel membrane. The unique feature of the device is that each microhabitat is physically confined suitable for both motile and non-motile cell culture, and at the same time, the device is transparent and can be perfused through the two side channels

amendable for precise environmental control of photosynthetic microorganisms. This microfluidic system is used to study the growth kinetics of a model microalgal strain, *Chlamydomonas reinhardtii* (*C. reinhardtii*), under ammonium (NH_4Cl) concentration gradients. Experimental results show that *C. reinhardtii* follows Monod growth kinetics with a half-saturation constant of $1.2 \pm 0.3 \mu\text{M}$. This microfluidic platform provides a fast (~ 50 fold speed increase), cost effective (less reagents and human intervention) and quantitative technique for microalgal growth studies, in contrast to the current chemostat or batch cell culture system. It can be easily extended to investigate growth kinetics of other microorganisms under either single or co-culture setting.

Introduction

Microalgae are microorganisms that use light energy to convert carbon dioxide and water into biomass and oxygen. They are critically important in both freshwater and marine ecosystems; they form the base of most aquatic food chains and reduce anthropogenic carbon dioxide emissions. They are also increasingly used in managed production systems for a wide range of products, including high-value food additives, pharmaceuticals, consumer products and biofuel.¹ Specifically they can be used to produce biologically active compounds such as antioxidants or antibacterial agents.^{2, 3} Microalgae are also attractive for biofuel production because of high areal productivity and because they do not compete with food crops for arable land or require increasingly scarce freshwater resources.⁴⁻⁷ While most algal species are benign, some produce toxins that can damage ecosystems and compromise drinking water.^{8, 9} Understanding what environmental triggers cause these species to bloom is critical to designing control

strategies for this global problem.⁹⁻¹³ Better tools to study algal growth kinetics thus can improve our understanding of algal populations in the natural environment as well as in managed engineered systems.

Current knowledge on microalgal growth is largely derived from field observation, raceway ponds, batch and chemostat systems.¹⁴⁻¹⁷ These tools are straightforward to use; however, they are not designed for efficient system parameter optimization. Although microfluidic models have been successful in studying roles of microenvironments in growth kinetics of many other cell types including bacteria and animal cells,¹⁸⁻²⁵ its applications for algal growth is still in early stage. Existing microfluidic models for algal growth studies are mostly droplet based, which afford a high throughput format, but they do not allow for continuous perfusion,^{6, 26 27, 28} which limits the dynamic environmental control. Micro-traps, on the other hand, allows for continuous perfusion,^{4, 5, 29} but are not suitable for motile cells or cells sensitive to shear stresses. A hybrid model of flow and diffusion-based microfluidic device has been used for toxicity screening of marine microalgae,³⁰ however, the system requires a three layer assembly, and is not designed for long term cell growth studies. In this article, we present a hydrogel-based array microhabitat system that uses agarose gel walls to provide cells with continuous nutrient supply via diffusion and yet protect the cells from the exposure to flow shear stress. This device is high throughput, straightforward to use, and it is applied to study the growth kinetics of a model microalgal strain, *C. reinhardtii*, under well controlled nitrogen gradients.

Experimental Methods

Silicon master fabrication

The silicon master mold was fabricated using the standard SU-8 negative resist photolithography technique at Cornell NanoScale Science & Technology Facility (CNF). A two-layer fabrication method was used to create the 200- μm -deep side channels and the 100- μm -deep array microhabitats. SU-8 2100 (MicroChem Corp., Westborough, MA) was first spun on a 100-mm

diameter and 525 ± 20 - μm -thick silicon wafer at 3,000 rpm for 30 s to form the first 100- μm -thick layer. After the edge bead removal, the resist went through a soft bake process. The purpose of the soft bake was to remove solvent in the resist film, and the slow ramping process was designed to avoid creating internal stresses within the resist layer. The soft bake steps are: (i) bake on a hotplate ramping up from room temperature to 65 °C in an hour; (ii) increase temperature further to 95 °C in another hour, and stay overnight at 95 °C; and (iii) cool down to room temperature. After the soft bake, the resist was exposed to a pattern of microhabitats and their supporting features using 365-nm i-line at 250 mJ/cm² on a contact aligner (ABM Contact Aligner, ABM, Inc, Silicon Valley, CA). The second layer of 100- μm -thick SU-8 2100 was spun, followed by edge bead removal and soft bake. The soft bake for the second layer also served as the post exposure bake for the first layer, which selectively crosslinks the exposed portion of the first-layer resist. After the post exposure bake, the exposed area of the first layer became visible, and was used in part as alignment marks for the alignment of the second layer. The both layers were exposed to a pattern of side channels using 320 mJ/cm² on the same contact aligner, followed by a post exposure bake identical to the soft bake described above. Both layers of the resist were then developed using SU-8 developer (MicroChem) until all the unexposed area was fully dissolved. After removing the SU-8 developer with isopropanol, a hard bake was performed in order to further crosslink the SU-8 features and anneal the minor cracks generated during the lithography process. For hard bake, a slow ramp up procedure was performed in an oven, and the temperature was ramped up to 200 °C from room temperature in a few hours and stayed at 200 °C for an hour, followed by natural cooling down to room temperature.

Microfluidic device assembly, cell seeding and flow control

The following is done to transfer the device pattern from the silicon master onto the agarose gel membrane. First, a boiled solution of 3% agarose (0.3 g agarose in 10 ml phosphate buffered

saline) was poured on the silicon master surrounded by a 1-mm-thick spacer in a laminar-flow hood. Second, the agarose solution was polymerized in room temperature in a few minutes. Finally, the polymerized agarose membrane was removed from the silicon master, and placed in media immediately for at least 45 minutes before final device assembly.

Before each experiment, a drop of 2 μl of *C. reinhardtii* (1×10^6 cell/ml) cell culture was placed on the patterned agarose gel membrane. The agarose gel membrane along with the spacer was then sandwiched between a Plexiglas manifold and a glass slide supported by a stainless steel frame (See Fig. 1). The cell numbers within each microhabitat ranged from 0 – 4 cells for habitat size of $100 \mu\text{m} \times 100 \mu\text{m} \times 100 \mu\text{m}$.

To control the flows along the two side channels, a syringe pump (KDS230, KD Scientific, Holliston, MA) together with a syringe (10 ml, BD, Franklin Lakes, NJ) was used. The inlets of the microfluidic device were connected to the syringe using a leveled gel-loading tip together with a medical grade tubing (ID = 0.25 mm, PharMed BPT, Cole-Parmer, Vernon Hills, IL). A flow rate of 0.7 $\mu\text{l}/\text{min}$ was used in our experiments. The entire setup was placed in a temperature and light controlled incubator (Percival Scientific, Perry, IA) where the device was enclosed in a glass beaker with water reservoirs to avoid drying.

Imaging and data analysis

All the images were taken with an epi-fluorescence microscope (Olympus IX51, Center Valley, CA), a CCD camera (Cascade 512B, Photometrics, Tucson, AZ), and an image acquisition software (IPLab imaging software, BD). For fluorescent imaging, a fluorescent light source (EXFO X-Cite 120 Fluorescence Illumination System, EXFO, Ontario, Canada), and a Cy5 filter cube (Semrock, Rochester, NY) were used.

Images were post-processed using image J (shareware from National Institute of Health). Cell numbers were counted using the built-in 'Find Maxima' function in image J and plotted as a

function of time in a semi-log plot. The specific growth rates were obtained from the fitted parameters of a linear fit to the exponential growth phase of the cell growth curve (typically, from 0.5 to 2.5 days). Statistical analyses were performed using Student t test with Prism (GraphPad Software, La Jolla, CA).

Cell culture and media

C. reinhardtii wild type strain CC-125 was obtained from the Stern Laboratory at the Boyce Thompson Institute of Plant Research at Cornell University. Cells were maintained in TAP (Tris Acetate Phosphate) medium (20 mM Tris, 17 mM Acetate, 0.68 mM K₂HPO₄, 7.26 mM KH₂PO₄, 7.5 mM NH₄Cl, and other salts including 0.34 mM CaCl₂) prepared using an established protocol³¹ with trace metal elements concentrations as described in Hutner et al.³² For microfluidic experiments, we used minimal medium, which was TAP without acetate for autotrophic cell growth. Prior to testing the culture in the microfluidic device, the strain was sub-cultured for three generations in minimal medium for autotrophic adaptation.³¹ Inoculum was prepared by adding 100 µl cell culture in an exponential phase to 5 ml fresh medium; the resulting cell density was approximately 1×10⁶ cell/ml. All *C. reinhardtii* cultures were incubated at 25°C, exposed to atmosphere and under a constant illumination of 80 µmol/m²-s. The cell density was monitored via measuring the chloroplast fluorescence with a 10-AU Fluorometer (Turner Designs, Sunnyvale, CA) during cell culture.

Results and Discussion

Experimental setup, device design and gradient characterization

The microfluidic setup was kept under an upside down Pyrex beaker with water reservoirs for humidity control (Fig. 1A), and imaged under a fluorescent microscope (Fig. 1B). Four identical

devices were patterned in a 1-mm-thin agarose gel membrane for parallel experiments. The agarose gel membrane was sandwiched between a Plexiglas manifold and a standard glass slide of 1 in \times 3 in in size, and supported by a stainless metal frame (See Fig. 1B and also ref. by Wong et al.³³). The key feature of each device was an array of microhabitats flanked by two side channels (Fig. 1C&D). The nutrient condition (e.g. nitrogen) within the array microhabitat was controlled by flowing nutrients/buffers through the source/sink channels respectively. This perfusion also allowed the system to stay wet, an important condition for keeping cells viable within microfluidic devices. Note that the nutrient concentrations of the microhabitats along the same column in the array were the same.

The design of the array can be easily reconfigured in our microfluidic platform for different purposes. We created arrays with 8 \times 8, 4 \times 4, and 2 \times 2 microhabitats, in which each habitat was a square with a side of 100, 200, and 600 μ m respectively. In all cases, the depth of the microhabitat was 100 μ m, the distance between two side channels was 2 mm and the microhabitat array was centered between the two side channels. An example of an 8 \times 8 array with a 100 μ m \times 100 μ m square habitat is shown in Fig. 1C&D. We note that the microfluidic platform can also be easily reconfigured for other functions. In Fig. S1, we show an array of microhabitats with interconnecting channels. This platform was limited to non-motile cell culture growth studies, but was compatible with an injection cell seeding method.

To characterize the chemical gradients established in the array area, we flowed 100 μ M fluorescein (molecular weight = 332 Da) solution and buffer along the source and sink channels respectively and took a sequence of fluorescent images. Fig. 1E is a fluorescent image of the array area of the device taken at $t = 1$ hr after the introduction of the flow. Fig. 1F demonstrates the fluorescent intensity profiles in the array area over time, showing that the system reaches a steady state in about 40 – 50 minutes. This is further verified in the dotted line of Fig. 1G when plotting

the fluorescent intensity in the middle of the array region as a function of time. To the first order and one-dimensional approximation, the time required to establish a steady fluorescein gradient is $t \approx l^2 / (2D)$ with $D = 5.21 \times 10^{-10} \text{ m}^2/\text{s}$ and $l = 2 \text{ mm}$, which is 64 min. This estimated gradient generation time is consistent with experimental results shown in Fig. 1F&G. Experimental results were further validated against results from COMSOL computation (See solid line in Fig. 1G).

Our array design (Fig. 1C&D) provides cell confinement for both motile and non-motile cells because microhabitats are not interconnected. This is important because many microalgae are highly motile.³⁴ The use of agarose gel allows us to separate the shear flows used for gradient generation from the cell culture within the microhabitat, eliminating the unwanted shear stress exposure to cells during experiments. This is critical for cell types such as microalgae that are sensitive to shear stress.¹³ Previously, agarose gel based microfluidic systems have been used successfully in our labs for cell chemotaxis studies.³⁵⁻³⁹ Here, we extend this technology by including the array format for high throughput microalgal growth studies. It should be noted that agarose gel is cheap, quick to polymerize and sterilize, and readily available in most biological labs. In addition, agarose gel is transparent allowing light to come through for photosynthetic microalgae. Lastly, because hydrogel walls surrounding the cell culture contain mostly water, the agarose-based device supports long-term cell culture with minimal humidity issues, in contrast to the PDMS device.^{36, 39, 40}

Baseline microalgal growth kinetics in the array microhabitat

Using the microfluidic device, we first studied growth kinetics of the microalga *C. reinhardtii* in the commonly used minimal medium (with ammonium as a nitrogen source). *C. reinhardtii* is a model algal strain for photosynthetic microorganism study, due to its fully sequenced genome, library of mutants, and well established cell culture procedures.⁴¹ In addition, its growth has been characterized extensively using conventional cell culture systems. We flowed minimal media

along both sink and source channels, and then took both bright field and fluorescent images of the microhabitat array every 24 hours. Cell growth with time within each habitat is clearly shown in Fig. 2A. Using the fluorescence images, we counted the cell numbers with image J. The resulted growth curves for three different microstat sizes all demonstrated an exponential growth phase followed by a stationary phase (See Fig. 2B). The slopes of the growth curves in the exponential region provided us the specific growth rates: 1.88 ± 0.09 ($600 \mu\text{m}$), 1.82 ± 0.17 ($200 \mu\text{m}$), and 1.79 ± 0.07 ($100 \mu\text{m}$) day^{-1} (Fig. 2B), which demonstrated that the growth rate was independent of the habitat size.

To obtain a control specific growth rate, we repeated similar experiments shown in Fig. 2A&B using minimal medium without nitrogen source. Fig. 2C shows the specific growth rates from 8 columns of the microhabitat array. The average specific rate is $1.12 \pm 0.02 \text{ day}^{-1}$, which is smaller than the rate obtained using minimal medium with nitrogen source. No statistical difference in specific growth rates among the different columns of microhabitats was observed indicating uniform nutrient distribution among habitats within the array. We note that cell growth curve in the minimal media without ammonium has a similar shape as those in Fig. 2B obtained with minimal media with ammonium, indicating that there is an internal nitrogen storage in the cell culture of *C. reinhardtii*.

The growth rate in the microhabitat using minimal medium reported here is consistent with the result of $1.47 \pm 0.30 \text{ day}^{-1}$ using conventional flask batch culture with the same media done in our lab (See Fig. S2) and others.⁴ In previous literature, the specific growth rate for *C. reinhardtii* using a microfluidic platform with convective flow and cell trap is reported to be 1.25 day^{-1} with the same minimal medium used as in our study.⁴ We note that the lower growth rate from a convective flow based microfluidic platform,⁴ in contrast to the result from our diffusion-based

microfluidic platform, is likely due to the influence of the shear flow and/or the loss of cells through the openings of the cell traps.

Microalgal growth under nitrogen gradients follows Monod kinetics

Nitrogen is essential for the synthesis of proteins and nucleic acids of microalgae. *C. reinhardtii* can assimilate different nitrogen sources, but the preferred one is ammonium due to its less demanding energetics.⁴² Here, we present studies of microalgal growth under gradients of ammonium concentration. *C. reinhardtii* was cultured in the array microhabitats under a 7.5 $\mu\text{M}/\text{mm}$ NH_4Cl gradient by flowing minimal medium with 15 μM NH_4Cl in source channel and minimal medium without NH_4Cl in the sink channel. The cell growth dependence on the NH_4Cl concentration was clearly demonstrated in Fig. 3A. Note cell number variations among habitats in each row are correlated to the initial cell seeding density. The cell growth rate at a specific NH_4Cl concentration was obtained using the growth curve of cells grown in a specific column of the array. Fig. 3B shows the specific growth rates at various NH_4Cl concentrations using combined data from three sets of experiments, with NH_4Cl concentration of 0 (control case), 2.25~12.75, and 112.5~637.5 μM . The control specific growth rate of $1.12 \pm 0.02 \text{ day}^{-1}$ in Fig. 3B is taken from Fig. 2C when cells grow in minimal medium without NH_4Cl .

The specific growth rate curve in Fig. 3B fits well to a modified Monod equation ($\mu = \mu_0 + \frac{\mu_{\text{max}} \cdot S}{K_s + S}$), where K_s is the half-saturation constant, μ is the specific growth rate (day^{-1}), μ_0 is the specific growth rate when the extracellular ammonium concentration is zero, $\mu_0 + \mu_{\text{max}}$ is the specific growth rate when ammonium is saturated, and S is the extracellular ammonium concentration. We obtained $K_s = 1.2 \pm 0.3 \mu\text{M}$ from the fitted values.

The growth kinetics shown in Fig. 3B demonstrates that ammonium critically regulates the growth of *C. reinhardtii*. In addition, it provides an important quantitative kinetic parameter, a half-saturation constant of ammonium with *C. reinhardtii*. To our knowledge, this is the first time

half-saturation constant of *C. reinhardtii* under ammonium gradients was obtained in experiments. This measurement demonstrates the enabling capability of quantitative measurements of microalgal growth kinetics using the microfluidic platform presented here. Previously, K_s values for marine phytoplankton species were reported to be in the range of 0.1~10 μM .¹⁴ In nature, nitrate concentration is reported to be 1~40 μM in freshwater throughout the US in 2002, according to National Atmospheric Deposition Program (NRSP-3) National Trends Network, which is consistent with the ammonium concentration reported here. We note that the ammonium concentration is typically ~ 10 mM in a batch culture medium; and ~10 μM in a chemostat culture medium.¹⁵

Inhibition of *C. reinhardtii* growth in millimolar range of ammonium

We measured specific growth rate of *C. reinhardtii* in the millimolar ranges of ammonium inspired by the fact that the widely used minimal medium contains 7.5 mM of ammonium.³¹ To our surprise, the specific growth rate decreases when the NH_4Cl concentration exceeded 1.0~2.0 mM (Fig. 4). The specific growth rate in Fig. 4 was obtained using data taken in array microhabitats with a NH_4Cl concentration gradient of 3.75 mM/mm.

Substrate inhibition with ammonium for the heterotrophic growth of *C. reinhardtii* with acetate was reported by Zhang et al. with an inhibition constant $K_i = 2.91 \text{ mM}$,¹⁶ but none exists for autotrophic growth. In ammonium transporter studies, it is reported that *C. reinhardtii* has eight putative ammonium transporters located at both the plasma and chloroplast membranes.⁴³ These transporters can be categorized into two classes: low- and high-affinity ammonium transporters. The high-affinity ammonium transporter functions at a low maximum uptake velocity when ammonium becomes limiting, while the low-affinity system has a high maximum uptake rate when nitrogen is replete.⁴⁴ The high-affinity ammonium transporters are known to be repressed by ammonium. Therefore, the substrate inhibition at high ammonium concentrations observed here is

not surprising. We note that the saturation of the specific growth rate starts around 10 μM of ammonium and the growth reduction occurs around 1 mM, spanning two orders of magnitude of ammonium concentration.

Heterogeneity of microalgal cell culture

The compatibility of the microfluidic device with an optical microscope enabled us to observe the heterogeneity of the microalgal cell culture. We observed that the individual cells have different morphologies, sizes, endogenous fluorescences, migration speeds, and growth rates within one population (See Fig. 5 and Movie S1). Fig. 5A shows the co-exiting of cell clusters and single cells within the same microhabitat. We further investigated the roles of initial cell number within each microhabitat in cell growth heterogeneity. Fig. 5B shows that cell growth rate has a large variation among various habitats when the initial cell number is 1, in contrast to the situation when the initial cell number is 3 or 4 within each habitat. The heterogeneous nature is consistent with the results from the cell growth of other microalgae in droplet cultures, showing that the growth rate of the cell culture starting with initial single cell seeding varies widely (0.55~1.52 day^{-1} with *C. vulgaris*).^{27,28}

One of the potential sources of the heterogeneity of *C. reinhardtii* is from its life cycle. *C. reinhardtii* has been known to proliferate in two ways: asexually and sexually. Under nitrogen starvation, vegetative cells are known to undergo haploid gametes.⁴⁵ In addition, deflagellation is a step in their life cycle when they divide, and daughter cells are not motile until they separate from the parental cell walls, which is one of the sources for motility variation. Our ongoing work in the lab has also pointed to a possible correlation between the cell clustering and cell-cell quorum sensing under specific environmental conditions. Taken together, the microfluidic platform presented here allows for the studies of heterogeneous nature of the microalgal cell

culture, which is critical for mechanistic studies of cell growth under controlled environmental conditions.

Conclusions and future perspective

We have developed an agarose-based array microhabitat system for microalgal growth studies with well defined chemical gradients. The unique features of the system are the microhabitat array format suitable for high throughput studies of microalgal cell growth under well controlled nutrient conditions, and a diffusion-based system for microalgal cells (both motile and non-motile) that are sensitive to flow shear. Using this system, we find that the specific growth rate of *C. reinhardtii* cultured on ammonium substrate follows Monod growth kinetics, with a half-saturation constant of $1.2 \pm 0.3 \mu\text{M}$. This work demonstrates the enabling capability of quantitative algal growth kinetics studies using a microfluidic platform. The tools developed here can be readily extended for studying environmental impacts on growth rate of other photosynthetic microorganisms.

Traditional microalgal cell culture systems can be broadly categorized into two types, batch and continuous system (e.g. chemostat). In comparison, micro-droplet based microfluidic systems represent the miniaturized batch cell culture system; while the presented hydrogel-based microhabitat array platform represents the advancement in the miniaturization of the continuous cell culture system. In contrast to the chemostat systems, the presented microfluidic platform is fast (about a 50 fold speed increases), and cost effective (requires much less human intervention and less reagents). In addition, it enables an ability to monitor cell heterogeneity at single cell level. For future development, we plan to use the microfluidic platform presented here for studying other cellular behavior including quorum sensing of photosynthetic microorganisms in single and co-culture setting.

Acknowledgements

This work was funded by the Academic Venter Fund from the Atkinson Center for a Sustainable Future and the New York State Hatch grant. MW and BJK thank Nelson G. Hairston, Jr., Hans Pearl and their research groups for insightful discussions. CKT thanks T. Pennell at Cornell NanoScale Science & Technology Facility (CNF) for the helpful discussions on microfabrication techniques.

Notes and references

^a Department of Biological and Environmental Engineering, Cornell University, Ithaca, NY, USA. Email: mw272@cornell.edu

†

Electronic Supplementary Information (ESI) available. See DOI: 10.1039/b000000x/

1. J. Delanoue and N. Depauw, *Biotechnol Adv*, 1988, 6, 725-770.
2. B. Metting and J. W. Pyne, *Enzyme Microb Tech*, 1986, 8, 386-394.
3. G. Rea, A. Antonacci, M. Lambrea, S. Pastorelli, A. Tibuzzi, S. Ferrari, D. Fischer, U. Johannmeier, W. Oleszek, T. Doroszewska, A. M. Rizzo, P. V. R. Berselli, B. Berra, A. Bertoli, L. Pistelli, B. Ruffoni, C. Calas-Blanchard, J. L. Marty, S. C. Litescu, M. Diaconu, E. Touloupakis, D. Ghanotakis and M. T. Giardi, *Trends Food Sci Tech*, 2011, 22, 353-366.
4. S. Bae, C. W. Kim, J. S. Choi, J. W. Yang and T. K. Seo, *Anal Bioanal Chem*, 2013, 405, 9365-9374.
5. H. S. Kim, T. L. Weiss, H. R. Thapa, T. P. Devarenne and A. Han, *Lab on a Chip*, 2014, 14, 1415-1425.
6. D. H. Lee, C. Y. Bae, J. I. Han and J. K. Park, *Anal Chem*, 2013, 85, 8749-8756.
7. J. W. Park, S. C. Na, T. Q. Nguyen, S. M. Paik, M. Kang, D. Hong, I. S. Choi, J. H. Lee and N. L. Jeon, *Biotechnol Bioeng*, 2015, 112, 494-501.
8. H. W. Paerl, N. S. Hall and E. S. Calandrino, *Sci Total Environ*, 2011, 409, 1739-1745.
9. H. W. Paerl and J. Huisman, *Science*, 2008, 320, 57-58.
10. D. J. Conley, H. W. Paerl, R. W. Howarth, D. F. Boesch, S. P. Seitzinger, K. E. Havens, C. Lancelot and G. E. Likens, *Science*, 2009, 323, 1014-1015.
11. K. Davidson, R. J. Gowen, P. Tett, E. Bresnan, P. J. Harrison, A. McKinney, S. Milligan, D. K. Mills, J. Silke and A. M. Crooks, *Estuar Coast Shelf S*, 2012, 115, 399-413.
12. W. E. A. Kardinaal, L. Tonk, I. Janse, S. Hol, P. Slot, J. Huisman and P. M. Visser, *Appl Environ Microb*, 2007, 73, 2939-2946.
13. P. H. Moisaner, J. L. Hench, K. Kononen and H. W. Paerl, *Limnol Oceanogr*, 2002, 47, 108-119.
14. R. W. Eppley, J. N. Rogers and J. J. McCarthy, *Limnol Oceanogr*, 1969, 14, 912-&.
15. N. Shtaida, I. Khozin-Goldberg, A. Solovchenko, K. Chekanov, S. Didi-Cohen, S. Leu, Z. Cohen and S. Boussiba, *J Exp Bot*, 2014, 65, 6563-6576.
16. X. W. Zhang, F. Chen and M. R. Johns, *Process Biochem*, 1999, 35, 385-389.
17. N. K. Singh and D. W. Dhar, *Agron. Sustain. Dev.*, 2011, 31, 605-629.
18. T. Ahmed, T. S. Shimizu and R. Stocker, *Integrative Biology*, 2010, 2, 604-629.
19. B. J. Kim and M. M. Wu, *Ann Biomed Eng*, 2012, 40, 1316-1327.
20. S. Kim, H. J. Kim and N. L. Jeon, *Integrative Biology*, 2010, 2, 584-603.
21. J. Wu, X. Wu and F. Lin, *Lab on a Chip*, 2013, 13, 2484-2499.
22. J. I. Betts and F. Baganz, *Microbial Cell Factories*, 2006, 5.
23. A. Groisman, C. Lobo, H. J. Cho, J. K. Campbell, Y. S. Dufour, A. M. Stevens and A. Levchenko, *Nat Methods*, 2005, 2, 685-689.
24. B. J. Kim, J. Diaio and M. L. Shuler, *Biotechnology Progress*, 2012, 28, 595-607.
25. K. S. Lee, P. Boccazzi, A. J. Sinskey and R. J. Ram, *Lab on a Chip*, 2011, 11, 1730-1739.
26. Y. Morimoto, W. H. Tan, Y. Tsuda and S. Takeuchi, *Lab on a Chip*, 2009, 9, 2217-2223.
27. A. Dewan, J. Kim, R. H. McLean, S. A. Vanapalli and M. N. Karim, *Biotechnol Bioeng*, 2012, 109, 2987-2996.
28. J. Pan, A. L. Stephenson, E. Kazamia, W. T. S. Huck, J. S. Dennis, A. G. Smith and C. Abell, *Integrative Biology*, 2011, 3, 1043-1051.
29. P. J. Graham, J. Riordon and D. Sinton, *Lab on a Chip*, 2015, DOI: 10.1039/C5LC00527B.
30. G. X. Zheng, Y. H. Wang, Z. M. Wang, W. L. Zhong, H. Wang and Y. J. Li, *Mar Pollut Bull*, 2013, 72, 231-243.
31. R. Togasaki, K. Brunke, M. Kitayama and O. M. Griffith, in *Progress in Photosynthesis Research*, ed. J. Biggins, Springer Netherlands, 1987, DOI: 10.1007/978-94-017-0516-5_106, ch. 106, pp. 499-502.
32. S. H. Hutner, *J Bacteriol*, 1946, 52, 213-221.
33. K. Wong, A. Ayuso-Sacido, P. Ahyow, A. Darling, J. A. Boockvar and M. Wu, *Journal of visualized experiments : JoVE*, 2008, DOI: 10.3791/674.
34. R. E. Goldstein, *Annu. Rev. Fluid Mech.*, 2015, 47, 343-375.
35. H. Chang, B. J. Kim, Y. S. Kim, S. S. Suarez and M. Wu, *PLoS ONE*, 2013, 8, e60587.
36. S. Y. Cheng, S. Heilman, M. Wasserman, S. Archer, M. L. Shuler and M. M. Wu, *Lab on a Chip*, 2007, 7, 763-769.
37. U. Haessler, Y. Kalinin, M. A. Swartz and M. W. Wu, *Biomed Microdevices*, 2009, 11, 827-835.
38. U. Haessler, M. Pisano, M. M. Wu and M. A. Swartz, *P Natl Acad Sci USA*, 2011, 108, 5614-5619.
39. B. J. Kim, P. Hannanta-anan, M. Chau, Y. S. Kim, M. A. Swartz and M. Wu, *PLoS ONE*, 2013, 8, e68422.
40. C. K. Tung, O. Krupa, E. Apaydin, J. J. Liou, A. Diaz-Santana, B. J. Kim and M. M. Wu, *Lab on a Chip*, 2013, 13, 3876-3885.
41. S. S. Merchant, S. E. Prochnik, O. Vallon, E. H. Harris, S. J. Karpowicz, G. B. Witman, A. Terry, A. Salamov, L. K. Fritz-Laylin, L. Maréchal-Drouard, W. F. Marshall, L.-H. Qu, D. R. Nelson, A. A. Sanderfoot, M. H. Spalding, V. V. Kapitonov, Q. Ren, P. Ferris, E. Lindquist, H. Shapiro, S. M. Lucas, J. Grimwood, J. Schmutz, P. Cardol, H. Cerutti, G. Chanfreau, C.-L. Chen, V. Cognat, M. T. Croft, R. Dent, S. Dutcher, E. Fernández, H. Fukuzawa, D. González-Ballester, D. González-Halphen, A. Hallmann, M. Hanikenne, M. Hippler, W. Inwood, K. Jabbari, M. Kalanon, R. Kuras, P. A. Lefebvre, S. D. Lemaire, A. V. Lobanov, M. Lohr, A. Manuell, I. Meier, L. Mets, M. Mittag, T. Mittelmeier, J. V. Moroney, J. Moseley, C. Napoli, A. M. Nedelcu, K. Niyogi, S. V. Novoselov, I. T. Paulsen, G. Pazour, S. Purton, J.-P. Ral, D. M. Riaño-Pachón, W. Riekhof, L. Rymarquis, M. Schroda, D. Stern, J. Umen, R. Willows, N. Wilson, S. L. Zimmer, J. Allmer, J. Balk, K. Bisova, C.-J. Chen, M. Elias, K. Gendler, C. Hauser, M. R. Lamb, H. Ledford, J. C. Long, J. Minagawa, M. D. Page, J. Pan, W. Pootakham, S. Roje, A. Rose, E. Stahlberg, A. M.

- Terauchi, P. Yang, S. Ball, C. Bowler, C. L. Dieckmann, V. N. Gladyshev, P. Green, R. Jorgensen, S. Mayfield, B. Mueller-Roeber, S. Rajamani, R. T. Sayre, P. Brokstein, I. Dubchak, D. Goodstein, L. Hornick, Y. W. Huang, J. Jhaveri, Y. Luo, D. Martínez, W. C. A. Ngau, B. Otilar, A. Poliakov, A. Porter, L. Szajkowski, G. Werner, K. Zhou, I. V. Grigoriev, D. S. Rokhsar and A. R. Grossman, *Science*, 2007, 318, 245-250.
42. F. J. Florencio and J. M. Vega, *Planta*, 1983, 158, 288-293.
43. E. Fernandez and A. Galvan, *J Exp Bot*, 2007, 58, 2279-2287.
44. A. Grossman, *Protist*, 2000, 151, 201-224.
45. R. Sager and S. Granick, *J Gen Physiol*, 1954, 37, 729-742.

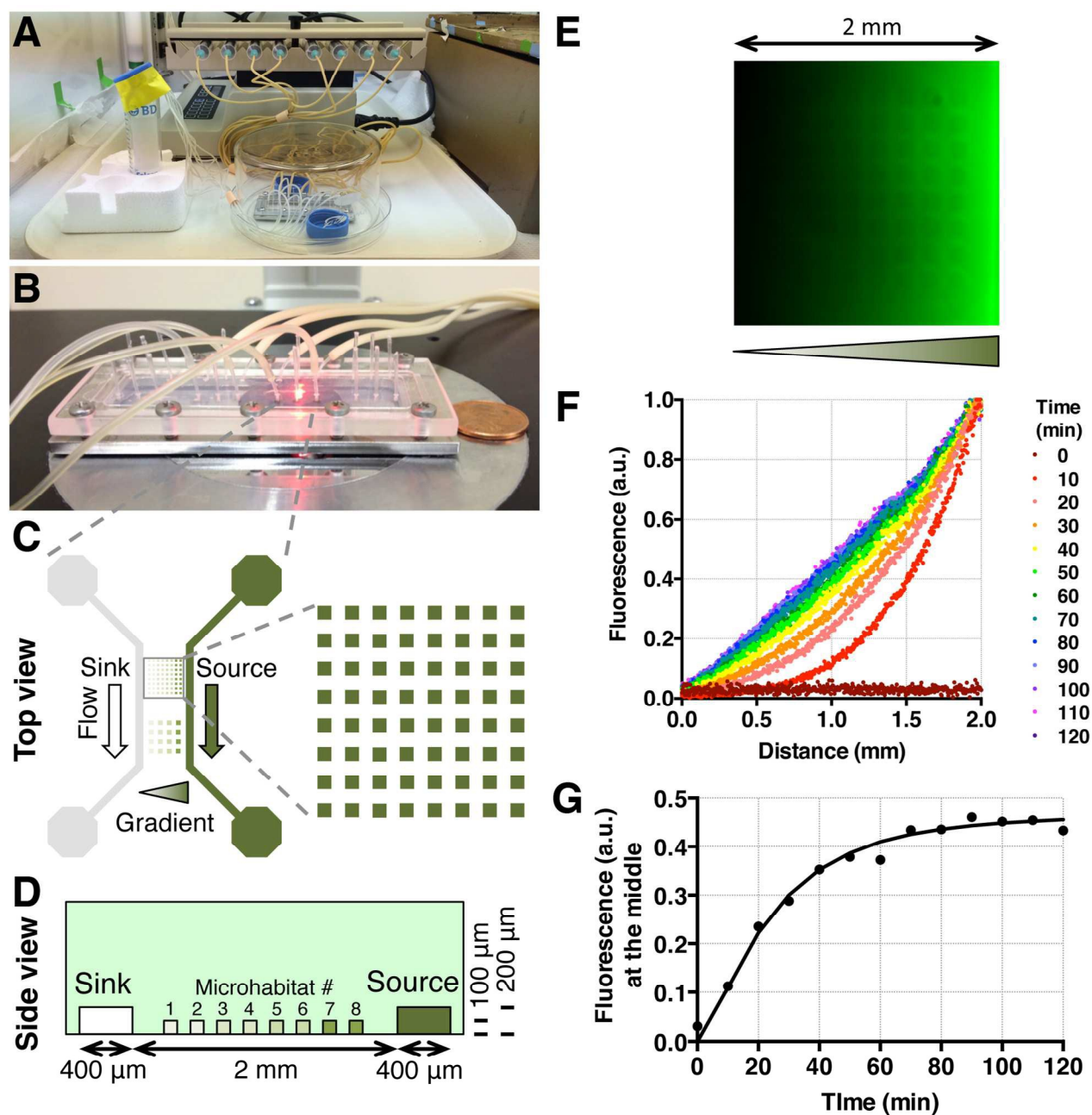


Fig. 1 Microfluidic platform design and gradient characterization. **A.** An image of the microfluidic platform under fluorescent light for the growth of photosynthetic microalgae. The microfluidic platform is enclosed in an upside down Pyrex container with water reservoirs for humidity control. A syringe pump is used to perfuse media through the device. **B.** An image of the microfluidic platform on a microscope stage. Each platform contains 4 individual devices patterned in an agarose gel membrane. Tubing is used for connecting to the syringe pump for flow control. **C.** Top view of a device. Nutrients/buffers flow through the two side channels and form a nutrient gradient in the microhabitat array area through molecular diffusion. Top array contains 64 microhabitats, each has a dimension of $100\ \mu\text{m} \times 100\ \mu\text{m} \times 100\ \mu\text{m}$, with a gap of $100\ \mu\text{m}$ between the two adjacent habitats. Bottom array contains 16 microhabitats, each has a dimension of $200\ \mu\text{m} \times 200\ \mu\text{m} \times 100\ \mu\text{m}$, with a gap of $200\ \mu\text{m}$. Cells are pre-seeded before sandwiching the agarose gel membrane between a plastic manifold and a glass slide. **D.** Side view of a

device. The distance between the source and sink channels is 2 mm, and the cross sectional area of each side channel is $400\ \mu\text{m} \times 200\ \mu\text{m}$. The nutrient concentration is the same for each column of the array, with the column number labeled. **E.** A fluorescence image of the array microhabitat taken at $t = 1\ \text{hr}$, where $t = 0$ is defined to be the time when fluorescein/buffer are introduced into the side channels. **F.** Time-evolution of fluorescence intensity profile in the array microhabitat area with a 10-min interval and total time duration of 120 min. Each colored line represents the fluorescence intensity profile at a time point. **G.** Experimental results (dotted line) are validated against that (solid line) from COMSOL computation. Time-evolution of fluorescence intensity in the middle of the array (or 1 mm away from sink channel).

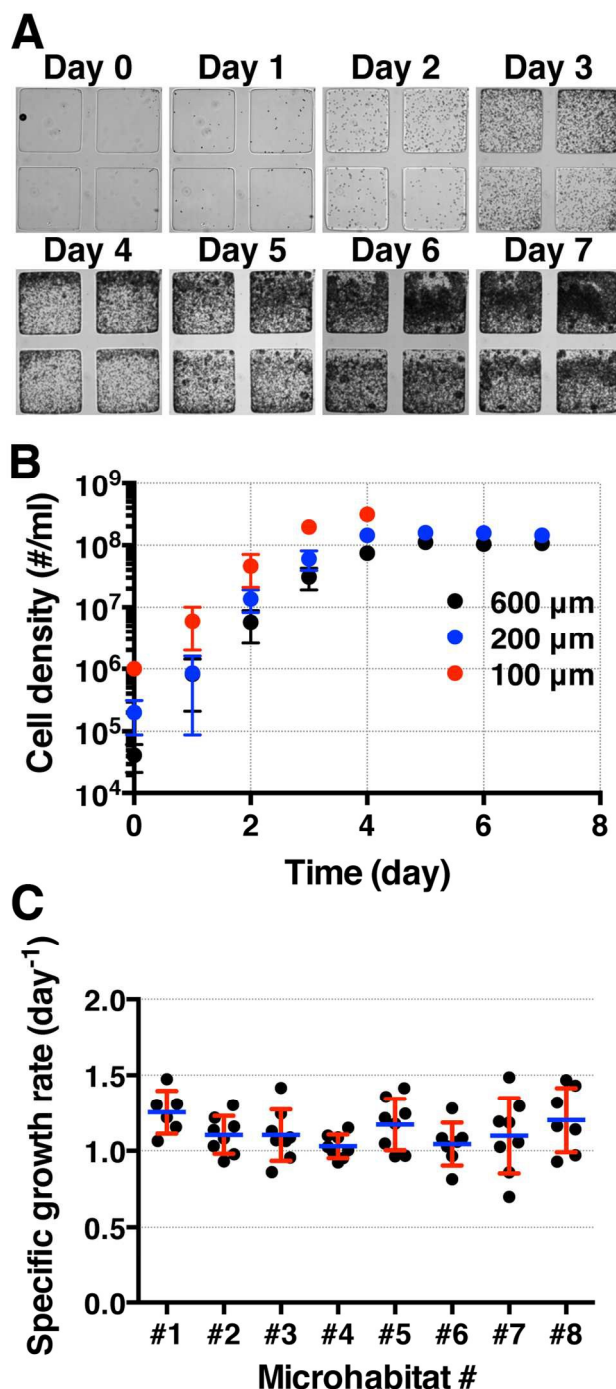


Fig. 2 Baseline microalgal growth kinetics within microhabitats with no gradients. **A.** Time evolution of bright field images of *C. reinhardtii* growing in microhabitat of size of $600 \mu\text{m} \times 600 \mu\text{m} \times 100 \mu\text{m}$ with minimal medium. **B.** Growth curves of cells in minimal medium, seeded in microhabitats of three different sizes. **C.** Specific growth rates of cells in minimal medium without NH_4Cl in individual microhabitats within the device (8×8 array of $100 \mu\text{m}$ size of microhabitat). Average specific growth rates along the specific column show that the basal growth rate is not statistical different throughout the rows.

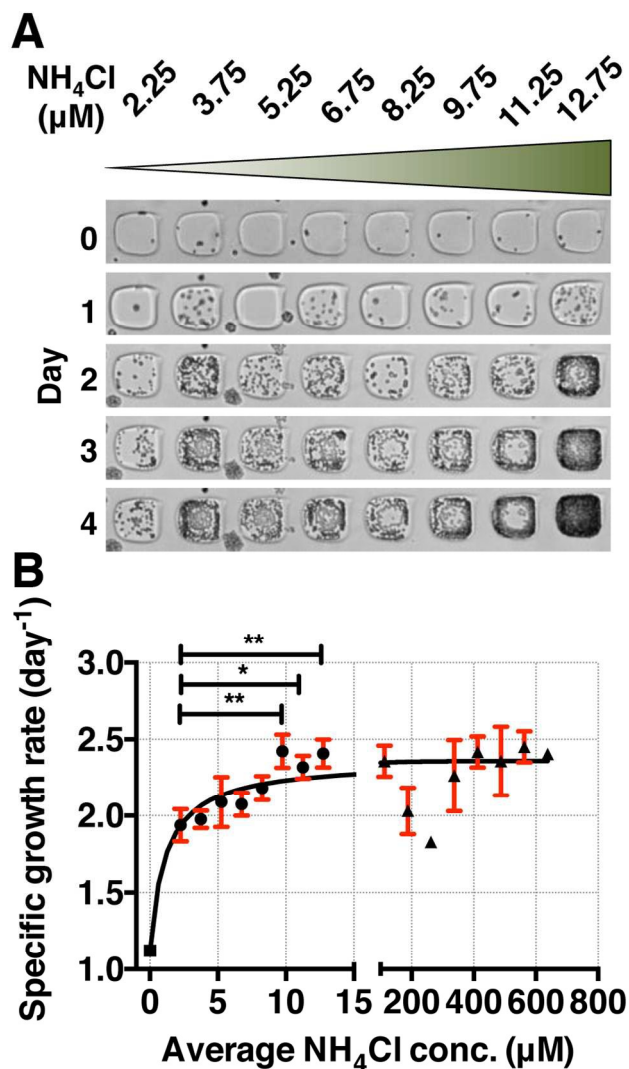


Fig. 3 Microalgal growth kinetics in spatial nitrogen gradients. **A.** Bright field images of one row of microhabitat over 4 days of time in the presence of NH₄Cl gradient of 7.5 μM/mm. **B.** Specific growth rate versus average NH₄Cl concentration. Square represents the control growth rate from data shown in Fig. 2C. Solid dots are a set of data taken in the presence of NH₄Cl gradient of 7.5 μM/mm. Triangles are a set of data taken in the presence of NH₄Cl gradient of 375 μM/mm. Solid line is a fit to modified Monod equation ($\mu = \mu_0 + \frac{\mu_{\max} S}{K_S + S}$). The fitted parameter gives the half-saturation coefficient K_S of 1.2 ± 0.3 μM.

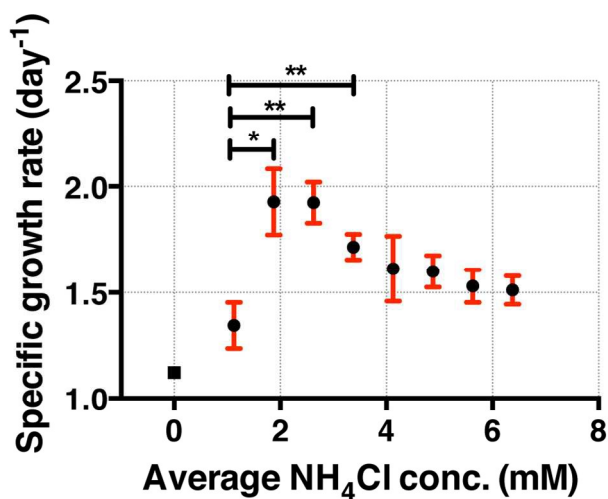


Fig. 4 Microalgal growth rate in millimolar nitrogen concentration regime. The specific growth rate of *C. reinhardtii* is reduced when the ammonium concentration is above 2 mM. Solid dots are data taken in the presence of 3.75 mM/mm NH₄Cl. The square data points in both graphs represents the average basal growth rate from all the microhabitats in Fig. 2C.

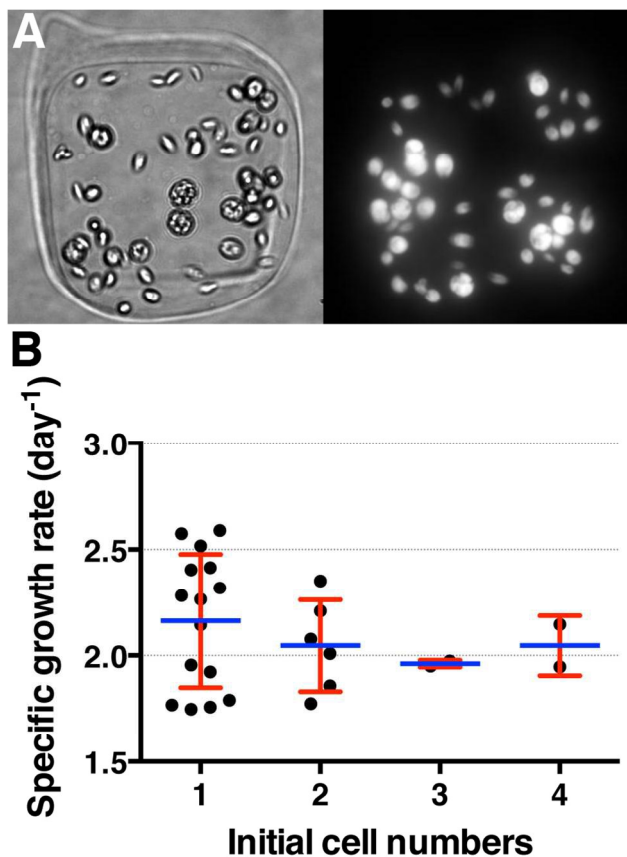


Fig. 5 Heterogeneity of cell morphology and growth. **A.** *C. reinhardtii* culture shows heterogeneous nature in a microhabitat of 100 μm size. Here cell cluster is observed alongside with single cells. **B.** Specific growth rate has a large variation among different microhabitats, but the average values do not depend on the initial cell numbers. Cells were cultured in the minimal medium with no gradient.